### Title

SILAC-Based Quantitative Proteomic Analysis Unveils Arsenite-Induced Perturbation of Multiple Pathways in Human Skin Fibroblast Cells.




### Journal

Chemical Research in Toxicology, 30(4)



### Authors

Zhang, Fan
Xiao, Yongsheng
Wang, Yinsheng



### Publication Date

2017-04-17

### DOI

10.1021/acs.chemrestox.6b00416

Peer reviewed

HHS Public Access

Author manuscript

*Chem Res Toxicol*. Author manuscript; available in PMC 2018 April 17.

Published in final edited form as:

*Chem Res Toxicol*. 2017 April 17; 30(4): 1006–1014. doi:10.1021/acs.chemrestox.6b00416.

# SILAC-Based Quantitative Proteomic Analysis Unveils Arsenite-Induced Perturbation of Multiple Pathways in Human Skin Fibroblast Cells

**Fan Zhang**, **Yongsheng Xiao**, and **Yinsheng Wang***

Department of Chemistry, University of California, Riverside, California 92521-0403, United States

## Abstract

Humans are exposed to arsenic species through inhalation, ingestion, and dermal contact, which may lead to skin, liver, and bladder cancers as well as cardiovascular and neurological diseases. The mechanisms underlying the cytotoxic and carcinogenic effects of arsenic species, however, remain incompletely understood. To exploit the mechanisms of toxicity of As(III), we employed stable isotope labeling by amino acids in cell culture (SILAC) together with LC/MS/MS analysis to quantitatively assess the As(III)-induced perturbation of the entire proteome of cultured human skin fibroblast cells. Shotgun proteomic analysis on an LTQ-Orbitrap Velos mass spectrometer facilitated the quantification of 3880 proteins, 130 of which were quantified in both forward and reverse SILAC-labeling experiments and displayed significant alterations (>1.5 fold) upon arsenite treatment. Targeted analysis on a triple-quadrupole mass spectrometer in multiple-reaction monitoring (MRM) mode confirmed the quantification results of some select proteins. Ingenuity pathway analysis revealed the arsenite-induced alteration of more than 10 biological pathways, including the Nrf2-mediated oxidative stress response pathway, which is represented by the upregulation of nine proteins in this pathway. In addition, arsenite induced changes in expression levels of a number of selenoproteins and metallothioneins. Together, the results from the present study painted a more complete picture regarding the biological pathways that are altered in human skin fibroblast cells upon arsenite exposure.

## Graphical abstract

*Corresponding Author: Phone: (951) 827-2700. Fax: (951) 827-4713. yinsheng.wang@ucr.edu.

**ORCID**

Yinsheng Wang: 0000-0001-5565-283X

**Notes**

The authors declare no competing financial interest.

Supporting Information

The Supporting Information is available free of charge on the ACS Publications website at DOI: 10.1021/acs.chemres-tox.6b00416. Protein quantification results, and lists of pathways, biological functions, and biological processes perturbed by As(III) treatment (PDF)

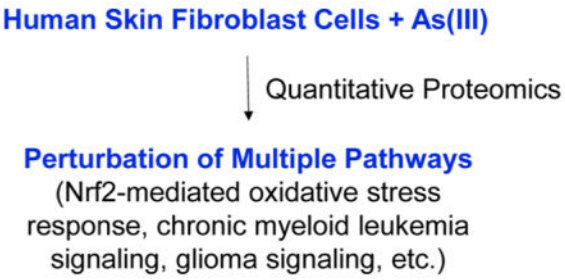


## INTRODUCTION

Arsenic is one of the most toxic elements in the environment, and human exposure to arsenic in drinking water is a widespread public health concern.[1] Epidemiological data from many regions around the world have revealed a strong correlation between high levels of arsenic in drinking water and cancer risk in humans.[2] Ingestion of high concentrations of arsenic is associated with elevated incidences of cancers of the skin, lung, and urinary bladder, and it is also a suspected cause of kidney and other malignancies.[3]

A number of studies have been conducted to explore the molecular mechanisms through which arsenic species exert their carcinogenic effects, and several modes of action have been proposed.[4] In this vein, trivalent arsenic [As(III)] is transported into mammalian cells through aquaglyceroporins AQP7 and AQP9.[5] Once it is inside the cell, arsenite is believed to increase cancer risk, in part by forming three-coordinate complexes with cysteine-containing proteins.[6,7] In addition, arsenic species may exert their carcinogenic effects by stimulating the formation of reactive oxygen species, inhibiting DNA damage repair, and modulating DNA and histone epigenetic marks.[4,8–12] Nevertheless, the mechanisms through which inorganic arsenite induces carcinogenesis remain incompletely understood.

Global gene expression analysis with microarray has been used for exploiting the molecular mechanisms action of inorganic arsenite, and it was found that 133 genes were differentially expressed upon arsenite treatment.[13] Although microarrays are widely used to monitor global changes in gene expression, the method affords limited information about alterations in protein expression.[14] The mass spectrometry (MS)-based proteomic method allows for the identification and quantification of a large number of proteins in complex samples. In this context, LC/MS/MS together with various stable isotope-labeling methods allows for the quantitative assessment of protein expression at the entire proteome scale. Stable isotope labeling by amino acids in cell culture (SILAC) is a simple and efficient labeling method with minimal bias, which can afford accurate quantification of subtle changes in protein abundance at the entire proteome level.[15]

Herein, we investigated, by employing SILAC in conjunction with LC/MS/MS analysis, the perturbation of the entire proteome of GM00637 human skin fibroblasts induced by arsenite treatment. We were able to quantify approximately 3880 unique proteins on an LTQ-Orbitrap Velos mass spectrometer, 130 of which were quantified in both forward and reverse SILAC-labeling experiments and displayed significant alterations upon arsenite treatment. We further validated the quantification results of some select proteins by targeted analysis in

multiple-reaction monitoring (MRM) mode on a triple-quadrupole mass spectrometer. The results from our study provide a better understanding about the biological pathways perturbed by arsenite treatment and about the mechanisms contributing to carcinogenic effects of arsenic.

## EXPERIMENTAL SECTION

### Cell Culture

GM00637 cells, which were kindly provided by Prof. Gerd P. Pfeifer (The City of Hope), were cultured in Dulbecco's modified Eagle's medium (DMEM) supplemented with 10% fetal bovine serum (FBS; Invitrogen, Carlsbad, CA), 100 IU/mL penicillin and 100 $\mu$g/mL of streptomycin in 75 $cm^2$ culture flasks. Cells were maintained in a humidified atmosphere with 5% $CO_2$ at 37 °C with medium renewal 2–3 times a week depending on cell density. For SILAC experiments, the complete light and heavy media were prepared by the addition of light or heavy lysine ([$^{13}C_6$, $^{15}N_2$]-L-lysine) and arginine ([$^{13}C_6$]-L-arginine), along with dialyzed FBS, to the DMEM medium without $_L$-lysine or $_L$-arginine (Cambridge Isotope Laboratories, Andover, MA). The GM00637 cells were cultured in heavy DMEM medium for at least 10 days to facilitate complete incorporation of the heavy lysine and arginine.

### $NaAsO_2$ Treatment and Sample Preparation

GM00637 cells, at a density of ~7 × $10^5$ cells/mL in light or heavy DMEM, were treated with 5 $\mu$M $NaAsO_2$ (Sigma, St. Louis, MO) for 24 h. The cells were subsequently harvested by centrifugation at 300*g* at 4 °C for 5 min and washed three times with ice-cold PBS. Cells were lysed with CelLytic M lysis buffer (Sigma) supplemented with 1 mM PMSF and a protease inhibitor cocktail (Sigma). The resulting cell lysate was centrifuged at 16,000*g* at 4 °C for 30 min, and the supernatant was collected. The protein concentration in the cell lysate was measured using Quick Start Bradford Protein Assay (Bio-Rad, Hercules, CA). In forward SILAC, the lysate of light labeled, arsenite-treated cells and that of the heavy labeled control cells were combined at a 1:1 ratio (w/w), and the labeling and arsenite treatment were reversed in the reverse SILAC experiment (Figure 1a).

### SDS-PAGE Separation and In-Gel Digestion

The above equi-mass mixture of light and heavy lysates was separated on a 12% SDS-PAGE with 4% stacking gel and stained with Coomassie blue. The gel was cut into 20 slices, and the proteins were reduced in-gel with dithiothreitol (DTT), alkylated with iodoacetamide (Sigma), and digested at 37 °C overnight with trypsin (Promega, Madison, WI) at an enzyme/substrate ratio of 1:100. Following the digestion, peptides were extracted from the gels with 5% acetic acid in $H_2O$ and then with 5% acetic acid in $CH_3CN/H_2O$ (1:1, v/v). The resulting peptide mixtures were dried in a SpeedVac concentrator and stored at –80 °C until further analysis.

### LC/MS/MS for Protein Identification and Quantification

Online LC/MS/MS analysis was performed on an LTQ-Orbitrap Velos mass spectrometer coupled with an EASY n-LCII HPLC system and a nanoelectrospray ionization source (Thermo, San Jose, CA), as described previously.[16] Briefly, the sample injection,

enrichment, desalting, and HPLC separation were conducted automatically on a homemade trapping column (150 μm × 40 mm) and separation column (75 μm × 200 mm, packed with ReproSil-Pur C18-AQ resin, 3 μm in particle size and 100 Å in pore size, Dr. Maisch HPLC GmbH, Germany). The peptide mixture was loaded onto the trapping column with a solvent mixture of 0.1% formic acid in $CH_3CN/H_2O$ (2:98, v/v) at a flow rate of 3.0 μL/min and subsequently separated with a 120 min linear gradient of 2–40% acetonitrile in 0.1% formic acid at a flow rate of 220 nL/min.

All tandem mass spectra were acquired in data-dependent scan mode. The full-scan mass spectra (from $m/z$ 350 to 2000) were acquired with a resolution of 60,000 at $m/z$ 400 after accumulation to a target value of 500,000. The 20 most abundant ions found in MS at a threshold above 500 counts were selected for fragmentation by low-energy collision-induced dissociation (CID) in the linear ion trap component of the instrument at a normalized collision energy of 35%. The same samples were also analyzed on the same instrument using higher energy collision-induced dissociation (HCD), which was performed by choosing the ten most abundant precursor ions for fragmentation in the HCD collision cell, where an activation time of 0.1 ms, an isolation window of 2.5 Da, and a normalized collision energy of 40% were used. The resolution for the HCD spectra was set to 7500 at $m/z$ 400.

The mass spectrometry proteomics data have been deposited to the ProteomeXchange Consortium via the PRIDE[17] partner repository with the data set identifier PXD005646.

## Data Processing

The LC/MS/MS data acquired from both low-energy CID and HCD were employed for the identification and quantification of the global proteome, which were conducted using Maxquant, version 1.2.0.18,[18] against UniProt human database (with 538,585 sequence entries, release date: 11.28.2012) to which contaminants and reverse sequences were added. The maximum number of miscleavages for trypsin was two per peptide. Cysteine carbamidomethylation and methionine oxidation were set as fixed and variable modifications, respectively. The tolerances in mass accuracy for MS and MS/MS were 25 ppm and 0.6 Da, respectively. Only those proteins with at least two distinct peptides being discovered from LC/MS/MS analyses were considered reliably identified. Proteins with significant changes in SILAC experiments were determined by a combination of ratio and ratio significance calculated by MaxQuant normalization under the assumption that the median of all log-transformed ratios is zero.[18] The required false-positive discovery rate was set to 1% at both the peptide and protein levels, and the minimal required peptide length was 6 amino acids. SILAC experiments were conducted in three biological replicates, including two forward and one reverse SILAC labelings. To establish the threshold ratios for determining the significantly changed proteins, we calculated the standard scores (z-scores) for protein ratios as described by Mann et al.[18,19] Our analysis showed that, at 95% confidence level, those proteins with expression ratios that are greater than 1.20 or less than 0.78 could be classified as significantly changed proteins. To be more stringent, however, we only considered a protein to be significantly changed if its differential expression ratio ($NaAsO_2$ treated/control) was greater than 1.5 or less than 0.67.

### Multiple-Reaction Monitoring (MRM) for Targeted Quantification of Select Proteins

Raw data generated from LTQ-Orbitrap Velos were searched using Mascot 2.2 (Matrix Science, London, U.K.). The resulting DTA files were employed as input for processing in Skyline[20] to generate a list of fragment ions derived from targeted peptides. Four fragment ion pairs were selected for MRM transitions of each targeted peptide.

The same SILAC samples analyzed on LTQ-Orbitrap Velos were subjected to analysis on a TSQ-Vantage triple quadrupole mass spectrometer (Thermo Fisher Scientific) equipped with an Accela HPLC system with split nanoflow. The flow rate was approximately 300 nL/min, and a linear gradient of 5–35% acetonitrile in 0.1% formic acid was used. A spray voltage of 1.8 kV and a capillary temperature of 200 °C were employed, and a resolution of 0.7 full-width at half-maximum (fwhm) was set for ion isolation in both Q1 and Q3. The collision gas pressure in Q2 was set at 1.2 mTorr, and a scan width of 0.2 $m/z$ and a cycle time of 5 s were used for data acquisition. Collision energy was optimized using the default setting in Skyline. Targeted peptides were quantified using Skyline, where the ratio of the light and heavy versions of each peptide was calculated from the mean ratios of peak areas found in the chromatograms for individual pairs of MRM transitions for the peptide.

### Ingenuity Pathway Analysis (IPA)

IPA (version 7.6, Ingenuity Systems Inc.) was employed to obtain information about relationships, functions, and pathways of the differentially regulated proteins, and the Ingenuity Knowledge Base (IPKB, Ingenuity Systems Inc.) was used.[21,22] The IPKB database contained gene regulatory and signaling pathways, which are integrated with other relevant databases including Gene Ontology (http://www.geneontology.org) and NCBI Gene (http://www.ncbi.nlm.nih.gov/gene). The proteins that were significantly changed upon $NaAsO_2$ treatment, including those quantified only in one cycle of the SILAC-labeling experiment, were included for the pathway analysis. IPA determines the interaction by calculating a significance score with Fisher's exact test and exporting it as a p-value; a p-value of $<0.05$ was considered significant for canonical pathways. Gene ontology analysis for significantly changed proteins was also conducted using DAVID Bioinformatics Resources, version 6.7 to reveal biological processes altered by arsenite exposure.[23]

## RESULTS AND DISCUSSION

To achieve a better understanding of the molecular mechanisms underlying the carcinogenic effects of arsenite, we set out to exploit the molecular targets and pathways affected by arsenite exposure. Toward this end, we employed an unbiased quantitative proteomic approach to assess the toxicant-induced alteration of the global proteome of GM00637 human skin fibroblast cells.

### $NaAsO_2$ Treatment and Protein Identification and Quantification

We first identified the optimal dose of $NaAsO_2$ by examining the survival of GM00637 cells upon treatment with different concentrations of $NaAsO_2$. Trypan blue exclusion assay results revealed approximately 5% cell death after a 24 h treatment with 5 $\mu$M $NaAsO_2$; however, cell viability was significantly diminished (by ~15%) after a similar treatment

using 10 μM $NaAsO_2$. Thus, we chose 5 μM $NaAsO_2$ for the subsequent experiments to minimize the cell death-induced alterations of protein expression. In this vein, the concentration of arsenic in groundwater can reach 5 μM in some heavily polluted areas in West Bengal, India.[1] In addition, humans in contaminated areas are exposed, albeit at lower concentrations, to arsenic species across the entire lifespan; such long-term exposure, however, cannot be practically implemented in model studies using cultured cells in a laboratory setting.

To obtain reliable quantification results, we conducted the SILAC experiments in three biological replicates, including two forward labelings and one reverse labeling (Figure 1a). LC/MS/MS analysis of these SILAC samples enabled us to identify more than 5000 proteins, 3880 of which were quantified with the expression ratio distribution shown in Figure 1b. Among these proteins, 2719 were quantified in all three SILAC-labeling experiments, and 2950 could be quantified in at least two SILAC labelings including the reverse cycle (Figure 1c). By employing two criteria, a protein (i) whose expression level has to change by at least 1.5 fold ($NaAsO_2$ treated/control) and (ii) has to be quantified in both forward and reverse SILAC-labeling experiments, we found that 130 proteins were significantly altered upon $NaAsO_2$ treatment. The results for all the quantified proteins and the proteins with significant changes are summarized in Tables S1 and S2, respectively. Shown in Figure 2a are the representative ESI-MS results for the quantification of ALFQDIK, a tryptic peptide derived from ferritin. The ESI-MS results demonstrated the arsenite-induced upregulation of ferritin in both forward and reverse SILAC-labeling experiments. In addition, MS/MS supported the identification of the light and heavy forms of this peptide (Figure 2b).

We next validated the quantification results of 50 select proteins by employing targeted analysis in MRM mode on a triple-quadrupole mass spectrometer, which was found to afford better sensitivity, reproducibility, and accuracy for quantification than the shotgun proteomics method based on data-dependent analysis.[24] It turns out that ~90% of the proteins displayed consistent quantification results with those obtained from data-dependent analysis on the LTQ-Orbitrap Velos mass spectrometer (Table S3). In this context, it is worth noting that, although both techniques revealed the significant upregulation of heme oxygenase 1, the expression ratio revealed by MRM-based targeted analysis (53.5-fold) was markedly higher than that determined by data-dependent analysis (16.6-fold). This is likely attributed to the somewhat limited dynamic range of quantification relying on MS data acquired on the Orbitrap Velos.

## Ingenuity Pathway Analysis (IPA) of Significantly Changed Proteins

We next performed IPA analysis to acquire information with respect to the relationships, functions, and pathways of the differentially expressed proteins induced by $NaAsO_2$ treatment.[25] The IPA results showed the alterations of several pathways, including the Nrf2-mediated oxidative stress response, pancreatic adenocarcinoma signaling, chronic myeloid leukemia signaling, cell cycle regulation, and IL-8 signaling (Table 2). In addition, the IPA results revealed several biological functions perturbed by $NaAsO_2$ treatment (Table S4). We also subjected the significantly changed proteins to DAVID analysis, which revealed a

number of biological processes that were altered upon arsenite exposure, including cellular responses to oxidative stress, cellular responses to cadmium ion, negative regulation of growth, chromosome segregation, and so forth (Table S5).

## $NaAsO_2$ Treatment Induced Upregulation of Nrf2-Mediated Oxidative Stress Response and IL-8 Signaling Pathways

The above IPA results showed that Nrf2-mediated oxidative stress response is one of the most significantly enriched pathways perturbed by $NaAsO_2$ treatment ($-\log P = 3.34$, Table 2), where nine proteins in this pathway were significantly altered upon $NaAsO_2$ treatment (Table 1). Oxidative stress occurs when the production of reactive oxygen species (ROS) in cells exceeds their detoxification capacity. Under normal physiological conditions, ROS form as byproducts of aerobic metabolism and play a crucial role in cell signaling and homeostasis.[26] Upon exposure to some environmental agents (e.g., UV light and heavy metal ions), ROS levels, however, can increase drastically in cells and result in damage to cellular components.[26] When cells are under oxidative stress, cytoplasmic Nrf2 protein is phosphorylated and translocated to the nucleus, where it can transactivate detoxifying and antioxidant enzymes, such as heme oxygenase 1 and superoxide dismutase.[27] Here, we found that $NaAsO_2$, when administered at 5 $\mu$M for 24 h, can result in markedly elevated expression of a hallmark protein of the Nrf2 pathway, i.e., heme oxygenase 1.[27] Other downstream target proteins related to the Nrf2 pathway, including ferritin, glutamate-cysteine ligase, heat shock protein 40, heat shock protein 70, and atypical protein kinase C, also displayed elevated expression upon $NaAsO_2$ treatment (Table 1).

Activation of the Nrf2 pathway is important in cellular defense against the deleterious effects of many environmental toxicants.[27] Natural Nrf2 activators (e.g., sulforaphane and *tert*-butylhydroquinone) have been suggested for dietary and therapeutic interventions against the adverse effects of arsenic,[28] and these activators act through a mechanism that depends on cysteine residue 151 (C151) in Keap1.[29] On the other hand, Nrf2 activation is also implicated in cancer promotion.[30] In this vein, a previous study showed that, unlike the natural Nrf2 activators, arsenite may trigger Nrf2 activation through a mechanism independent of C151 in Keap1.[31] In particular, arsenic may trigger Nrf2 activation via p62 accumulation, which induces autophagy dysregulation and Keap1 sequestration.[32] The latter hampers the Keap1-Cullin 3 E3 ubiquitin ligase-mediated ubiquitination of Nrf2, thereby impeding the degradation of Nrf2 by the proteasomal pathway.[32] Thus, different from the protective effects of the natural Nrf2 activators, prolonged Nrf2 activation emanating from arsenite exposure has the potential to elicit toxicity and carcinogenicity.[32]

Our IPA results of the quantitative proteomic data also unveiled perturbation of the IL-8 signaling pathway. This finding parallels previous observations that arsenite exposure could result in elevated expression of IL-8 and other proinflammatory cytokines (i.e., IL-6 and IL-1$\beta$) in human bronchial epithelial cells.[33,34] In addition, IL-6 and IL-8 were found to be essential for the malignant progression of arsenite-transformed human bronchial epithelial cells,[33] and arsenite exposure was thought to stimulate the expression of the IL-8 gene through stabilization and transactivation of HIF-2$\alpha$[33] or through low levels of constitutive nuclear NF-$\kappa$B.[34]

### $NaAsO_2$-Induced Downregulation of Selenoproteins

We observed significantly diminished expression of a group of selenoproteins, including glutathione peroxidase 4 (GPx4) and selenoproteins H, K, M, and S (Table 1). These proteins are known to play pivotal roles in antioxidant responses. For instance, glutathione peroxidases, which harbor a selenocysteine at their active sites, catalyze the decomposition of harmful hydroperoxides.[35] The importance of GPx4 in cellular antioxidant defense response is manifested by the observation that GPx4 KO mice displayed higher sensitivity to oxidative stress forged by ionizing radiation and $H_2O_2$.[36] Additionally, cells with reduced glutathione peroxidase level or activity exhibited higher sensitivity toward arsenite.[37] Selenoprotein K (SelK) is also involved in protecting cells from the deleterious effects of ROS.[38] In addition, selenoprotein H (SelH) was found to be important in regulating de novo glutathione synthesis and phase-II detoxification,[39] whereas selenoprotein S (SelS) could modulate ER stress and was responsible for the control of inflammatory response.[40]

Interestingly, all the above selenoproteins carry a selenocysteine that is capable of binding As(III) in cells.[6] Moreover, arsenite is known to induce the decreased expression of GPx, a situation that diminishes the cell's ability to defend against ROS.[41] Thus, the decreased expression of all the quantified selenoproteins indicates that arsenite may elicit its cytotoxic effect partly through perturbation of selenoprotein synthesis and/or covalently binding to selenocysteines in these proteins, both of which reduce the cells' capacity for defending against oxidative stress. In addition, the reduced expression of selenoproteins in GM00637 human skin fibroblast cells is consistent with previous findings made with human keratinocytes and mouse embryonic stem cells exposed with arsenite.[41,42] These results suggest that the alteration in expression of these selenoproteins might be a general effect of arsenite exposure.

### $NaAsO_2$ Induced Upregulation of Metallothionein (MT) Proteins

$NaAsO_2$ treatment also gave rise to considerable increases in the expression levels of MT proteins, including metallothioneins 1F, 1H, 1X, and 2 (Table 1). MTs are a family of low-molecular weight polypeptides with 20–30% of amino acids being cysteines.[43] Our results are in keeping with the previous finding that As(III) could induce the expression of MT proteins in mice[44] and with the fact that these proteins are able to bind to a variety of heavy metals and metalloids including cadmium, copper, arsenic, and zinc through their cysteine-rich domain.[45,46]

### $NaAsO_2$ Treatment Induced Alteration of Zinc-Finger Proteins

Zinc-finger proteins are characterized by their capability to coordinate with one or more zinc ions to stabilize their structures.[47] RING finger, a protein structural domain of the zinc-finger type with a $Cys_3HisCys_4$ amino acid motif, is present in the majority of E3 ubiquitin ligases.[48] In this context, As(III) was found to bind to the RING finger domain of PML in the oncogenic PML-RAR$\alpha$ fusion protein, and this binding ultimately results in the proteasomal degradation of the fusion protein.[49] In addition, we observed recently that As(III) could bind to the RING finger domain of RNF20/RNF40 histone E3 ubiquitin ligase, which diminishes its capability in ubiquitinating histone H2B at lysine 120, thereby creating a chromatin environment that is not conducive for DNA double strand break repair.[10]

Moreover, As(III) could inhibit the oxidation of 5-methylcytosine in DNA via binding to the zinc finger motifs of ten-eleven translocation (Tet) family enzymes and suppressing their enzymatic activities,[11] and As(III) exposure was found to compromise the repair of oxidatively generated DNA lesions through binding to the zinc finger domain of poly(ADP-ribose) polymerase-1.[50,51]

We found that a number of zinc-finger proteins were differentially expressed upon arsenite treatment. In particular, E3 ubiquitin-protein ligases UBR1, UBR3, and UBR7 were substantially downregulated. UBR family proteins are also known as N-recognins due to the recognition of N-degrons or N-degron-like molecules in the N-end rule pathway,[52] which functions in the control of peptide import,[53] chromosome segregation,[54] apoptosis[55] and cardiovascular development.[56] UBR1 recognizes type 1 and type 2 N-termini, whereas the recognition sites for UBR3 and UBR7 remain unclear.[57] UBR3 was shown recently to polyubiquitinate APE1, a protein involved in DNA repair and transcriptional regulation.[58] UBR7, a novel protein carrying a RING finger-like PHD domain, is known to be associated with transcriptional regulation.[59] Owing to the important role of these RING-finger or RING-finger-like proteins in cell cycle, DNA damage repair, and transcriptional regulation,[47] our quantification results indicate that arsenite may affect these biological processes and induce its carcinogenic effect through altering the expression of RING-finger domain-containing proteins.

## CONCLUSIONS

Arsenic is an important human carcinogen, and human exposure to arsenicals in drinking water is known to be associated with the development of cancers of the skin, lung, urinary bladder, liver, and kidney. Although accumulating evidence indicates that arsenic exposure could lead to chromosomal abnormalities, oxidative stress, altered DNA repair, and cell cycle arrest,[6] few studies have been carried out to comprehensively examine the alterations in expression of proteins involved in these processes.[60]

In the present study, we quantitatively assessed the sodium arsenite-induced perturbation of the entire proteome of GM00637 human skin fibroblast cells. Our results showed that more than 250 proteins were significantly altered upon a 24 h treatment with 5 $\mu$M $NaAsO_2$. Among these 250 proteins, 130 were quantified in both forward and reverse SILAC-labeling experiments. IPA analysis of the significantly changed proteins revealed that arsenite exposure gave rise to the perturbation of more than ten pathways, including Nrf2-mediated oxidative stress response, pancreatic adenocarcinoma signaling, and cell cycle regulation, to name a few. In light of previous findings about the effects of As(III) binding on the disruption of enzymatic activities of other RING finger E3 ubiquitin ligases,[10,49] we reason that the As(III)-induced activation of Nrf2 pathway may occur through the binding of As(III) to the RING finger protein (i.e., RBX1) of the cullin 3 (CUL3) E3 ubiquitin ligase complex, which was found previously to be crucial in the ubiquitination and subsequent proteasomal degradation of Nrf2.[61] In this vein, it is worth noting that the expression level of CUL3 or RBX1 was not altered after As(III) exposure (Table S1). This is not surprising in light of our previous findings that As(III) could disrupt the activities of RNF20/RNF40 E3 ubiquitin ligase and Tet family of enzymes without altering the expression levels of these proteins,

suggesting that the binding alters the conformations of these enzymes and thus compromises their enzymatic activities.[10,11] It will be important to examine the binding between As(III) and the RBX1 protein in the CUL3 E3 ubiquitin ligase complex and the effect of the binding on its E3 ligase activity in the future.

Although some of these pathways were identified in previous studies, our unbiased quantitative proteomic approach led to the discovery of the differential expression of many proteins involved in each of these pathways. Thus, the current study paints a more complete picture for $NaAsO_2$-induced alterations of cellular pathways and provides important new knowledge for understanding the implications of arsenic exposure in the development of cancer in the skin and other tissues.[3] In this regard, it is worth comparing the results made from the present study with a previous study with the use of HL-60 acute promyelocytic leukemia cells.[60] In that study, we observed that arsenite treatment led to a reduced level of fatty acid synthase, and the arsenite-induced growth inhibition of HL-60 cells could be rescued by treatment with palmitate, the final product of fatty acid synthase, suggesting that arsenite exerts its cytotoxic effect in acute promyelocytic leukemic cells, in part by suppressing the expression of fatty acid synthase and inhibiting the endogenous production of fatty acid.[60] This difference is likely attributed to the differences between cancer and normal cells, where fatty acid synthase is known to be expressed at high levels in cancer cells, including HL-60 cells.[62]

It is worth discussing the observations made from the present study with a previously published microarray study by Yih et al.,[13] where the expression profiles of 568 human genes in HFW cells, derived from human newborn foreskin, were monitored after exposure to 5 $\mu$M arsenite for 0, 1, 2, 4, 8, 16, and 24 h. In that study, the authors divided the genes into six clusters according to their temporal expression profiles, where clusters I and II contained 25 and 24 genes displaying high (cluster 1) or moderate (cluster 2) increases in expression at all time points following arsenite treatment. Our quantitative proteomic experiments facilitated us to quantify six proteins for those genes in cluster 1, i.e., NRAS, SRPK1, CCNB, HSPA1, HSPD1, and NAT1, with expression ratios in arsenite-treated/control cells being 1.01 ± 0.10, 0.98 ± 0.09, 1.32 ± 0.29, 2.23 ± 0.47, 1.46 ± 0.33, and 1.06, respectively (Table S1). We also quantified four proteins for those genes in cluster 2, i.e., ABL1, FADD, PPP1CB, and NIT1, with expression ratios being 5.57, 1.04 ± 0.06, 0.82 ± 0.42, and 0.77 ± 0.07, respectively (Table S1). Thus, among these 10 commonly quantified gene products, only HSPA1, HSPD1, and ABL1 display increased expression at both mRNA and protein levels. Examination of commonly quantified gene products in other clusters also revealed the lack of significant changes in expression levels of proteins for those genes where microarray-based gene expression analysis unveiled a substantial change in mRNA expression (data not shown). The cell lines used in the two studies are not identical (although both were fibroblasts derived from human skin), which may contribute partly to differences made from the mRNA and protein expression analyses. Moreover, inconsistences in findings made from transcriptomics and proteomics studies are well documented in the literature,[63] which are not surprising from the viewpoint that, aside from transcriptional regulation, steady-state protein levels in cells are subjected to post-transcriptional and translational regulations and are modulated by protein degradation pathways.[63] The results from the present study also demonstrated that the SILAC-based quantitative proteomic

analysis constitutes a powerful tool for the unbiased discovery of cellular pathways altered upon exposure to an environmental toxicant (i.e., arsenic).

## Supplementary Material

Refer to Web version on PubMed Central for supplementary material.

## Acknowledgments

**Funding**

This work was supported by the National Institutes of Health (R01 ES019873).

## ABBREVIATIONS

| | |
|---|---|
| **SILAC** | stable isotope labeling by amino acids in cell culture |
| **MRM** | multiple-reaction monitoring |
| **MS** | mass spectrometry |
| **ROS** | reactive oxygen species |
| **GPx4** | glutathione peroxidase 4 |
| **CUL3** | cullin 3 |

## References

1. Das D, Chatterjee A, Samanta G, Mandal B, Chowdhury TR, Chowdhury PP, Chanda C, Basu G, Lodh D, et al. Arsenic contamination in groundwater in six districts of West Bengal, India: the biggest arsenic calamity in the world. Analyst. 1994; 119:168N–170N.
2. Cantor KP, Lubin JH. Arsenic, internal cancers, and issues in inference from studies of low-level exposures in human populations. Toxicol Appl Pharmacol. 2007; 222:252–257. [PubMed: 17382983]
3. Hughes MF. Arsenic toxicity and potential mechanisms of action. Toxicol Lett. 2002; 133:1–16. [PubMed: 12076506]
4. Kitchin KT. Recent advances in arsenic carcinogenesis: modes of action, animal model systems, and methylated arsenic metabolites. Toxicol Appl Pharmacol. 2001; 172:249–261. [PubMed: 11312654]
5. Liu Z, Shen J, Carbrey JM, Mukhopadhyay R, Agre P, Rosen BP. Arsenite transport by mammalian aquaglyceroporins AQP7 and AQP9. Proc Natl Acad Sci U S A. 2002; 99:6053–6058. [PubMed: 11972053]
6. Kitchin KT, Wallace K. The role of protein binding of trivalent arsenicals in arsenic carcinogenesis and toxicity. J Inorg Biochem. 2008; 102:532–539. [PubMed: 18164070]
7. Shen S, Li XF, Cullen WR, Weinfeld M, Le XC. Arsenic binding to proteins. Chem Rev. 2013; 113:7769. [PubMed: 23808632]
8. Liu SX, Athar M, Lippai I, Waldren C, Hei TK. Induction of oxyradicals by arsenic: implication for mechanism of genotoxicity. Proc Natl Acad Sci U S A. 2001; 98:1643–1648. [PubMed: 11172004]
9. Wang F, Zhou X, Liu W, Sun X, Chen C, Hudson LG, Liu KJ. Arsenite-induced ROS/RNS generation causes zinc loss and inhibits the activity of poly (ADP-ribose) polymerase-1. Free Radical Biol Med. 2013; 61:249. [PubMed: 23602911]
10. Zhang F, Paramasivam M, Cai Q, Dai X, Wang P, Lin K, Song J, Seidman MM, Wang Y. Arsenite binds to the RING finger domains of RNF20-RNF40 histone E3 ubiquitin ligase and inhibits DNA double-strand break repair. J Am Chem Soc. 2014; 136:12884–12887. [PubMed: 25170678]

11. Liu S, Jiang J, Li L, Amato NJ, Wang Z, Wang Y. Arsenite targets the zinc finger domains of Tet proteins and inhibits Tet-mediated oxidation of 5-methylcytosine. Environ Sci Technol. 2015; 49:11923–11931. [PubMed: 26355596]
12. Howe CG, Liu X, Hall MN, Slavkovich V, Ilievski V, Parvez F, Siddique AB, Shahriar H, Uddin MN, Islam T, Graziano JH, Costa M, Gamble MV. Associations between Blood and Urine Arsenic Concentrations and Global Levels of Post-Translational Histone Modifications in Bangladeshi Men and Women. Environ Health Perspect. 2016; doi: 10.1289/ehp.1510412
13. Yih LH, Peck K, Lee TC. Changes in gene expression profiles of human fibroblasts in response to sodium arsenite treatment. Carcinogenesis. 2002; 23:867–876. [PubMed: 12016162]
14. Russo G, Zegar C, Giordano A. Advantages and limitations of microarray technology in human cancer. Oncogene. 2003; 22:6497–6507. [PubMed: 14528274]
15. Ong SE, Blagoev B, Kratchmarova I, Kristensen DB, Steen H, Pandey A, Mann M. Stable isotope labeling by amino acids in cell culture, SILAC, as a simple and accurate approach to expression proteomics. Mol Cell Proteomics. 2002; 1:376–386. [PubMed: 12118079]
16. Zhang F, Dai X, Wang Y. 5-Aza-2′-deoxycytidine induced growth inhibition of leukemia cells through modulating endogenous cholesterol biosynthesis. Mol Cell Proteomics. 2012; 11:M111.016915.
17. Vizcaino JA, Csordas A, Del-Toro N, Dianes JA, Griss J, Lavidas I, Mayer G, Perez-Riverol Y, Reisinger F, Ternent T, Xu QW, Wang R, Hermjakob H. 2016 update of the PRIDE database and its related tools. Nucleic Acids Res. 2016; 44:11033. [PubMed: 27683222]
18. Cox J, Mann M. MaxQuant enables high peptide identification rates, individualized p.p.b.-range mass accuracies and proteome-wide protein quantification. Nat Biotechnol. 2008; 26:1367–1372. [PubMed: 19029910]
19. Graumann J, Hubner NC, Kim JB, Ko K, Moser M, Kumar C, Cox J, Scholer H, Mann M. Stable isotope labeling by amino acids in cell culture (SILAC) and proteome quantitation of mouse embryonic stem cells to a depth of 5,111 proteins. Mol Cell Proteomics. 2008; 7:672–683. [PubMed: 18045802]
20. MacLean B, Tomazela DM, Shulman N, Chambers M, Finney GL, Frewen B, Kern R, Tabb DL, Liebler DC, MacCoss MJ. Skyline: an open source document editor for creating and analyzing targeted proteomics experiments. Bioinformatics. 2010; 26:966–968. [PubMed: 20147306]
21. Muller T, Schrotter A, Loosse C, Helling S, Stephan C, Ahrens M, Uszkoreit J, Eisenacher M, Meyer HE, Marcus K. Sense and nonsense of pathway analysis software in proteomics. J Proteome Res. 2011; 10:5398–5408. [PubMed: 21978018]
22. Thomas S, Bonchev D. A survey of current software for network analysis in molecular biology. Hum Genomics. 2010; 4:353–360. [PubMed: 20650822]
23. Huang DW, Sherman BT, Lempicki RA. Systematic and integrative analysis of large gene lists using DAVID bioinformatics resources. Nat Protoc. 2008; 4:44–57.
24. Lange V, Picotti P, Domon B, Aebersold R. Selected reaction monitoring for quantitative proteomics: a tutorial. Mol Syst Biol. 2008; 4:222. [PubMed: 18854821]
25. Mayburd AL, Martinez A, Sackett D, Liu HT, Shih J, Tauler J, Avis I, Mulshine JL. Ingenuity network-assisted transcription profiling: Identification of a new pharmacologic mechanism for MK886. Clin Cancer Res. 2006; 12:1820–1827. [PubMed: 16551867]
26. Finkel T, Holbrook NJ. Oxidants, oxidative stress and the biology of ageing. Nature. 2000; 408:239–247. [PubMed: 11089981]
27. Kensler TW, Wakabayashi N, Biswal S. Cell survival responses to environmental stresses via the Keap1-Nrf2-ARE pathway. Annu Rev Pharmacol Toxicol. 2007; 47:89–116. [PubMed: 16968214]
28. Wang XJ, Sun Z, Chen W, Eblin KE, Gandolfi JA, Zhang DD. Nrf2 protects human bladder urothelial cells from arsenite and monomethylarsonous acid toxicity. Toxicol Appl Pharmacol. 2007; 225:206–213. [PubMed: 17765279]
29. Lau A, Whitman SA, Jaramillo MC, Zhang DD. Arsenic-mediated activation of the Nrf2-Keap1 antioxidant pathway. J Biochem Mol Toxicol. 2013; 27:99–105. [PubMed: 23188707]
30. Lau A, Villeneuve NF, Sun Z, Wong PK, Zhang DD. Dual roles of Nrf2 in cancer. Pharmacol Res. 2008; 58:262–270. [PubMed: 18838122]

31. Wang XJ, Sun Z, Chen W, Li Y, Villeneuve NF, Zhang DD. Activation of Nrf2 by arsenite and monomethylarsonous acid is independent of Keap1-C151: enhanced Keap1-Cul3 interaction. Toxicol Appl Pharmacol. 2008; 230:383–389. [PubMed: 18417180]
32. Lau A, Zheng Y, Tao S, Wang H, Whitman SA, White E, Zhang DD. Arsenic inhibits autophagic flux, activating the Nrf2-Keap1 pathway in a p62-dependent manner. Mol Cell Biol. 2013; 33:2436–2446. [PubMed: 23589329]
33. Xu Y, Zhao Y, Xu W, Luo F, Wang B, Li Y, Pang Y, Liu Q. Involvement of HIF-2a-mediated inflammation in arsenite-induced transformation of human bronchial epithelial cells. Toxicol Appl Pharmacol. 2013; 272:542–550. [PubMed: 23811328]
34. Jaspers I, Samet JM, Reed W. Arsenite exposure of cultured airway epithelial cells activates kB-dependent interleukin-8 gene expression in the absence of nuclear factor-kB nuclear translocation. J Biol Chem. 1999; 274:31025–31033. [PubMed: 10521501]
35. Imai H, Nakagawa Y. Biological significance of phospholipid hydroperoxide glutathione peroxidase (PHGPx, GPx4) in mammalian cells. Free Radical Biol Med. 2003; 34:145–169. [PubMed: 12521597]
36. Imai H, Hirao F, Sakamoto T, Sekine K, Mizukura Y, Saito M, Kitamoto T, Hayasaka M, Hanaoka K, Nakagawa Y. Early embryonic lethality caused by targeted disruption of the mouse PHGPx gene. Biochem Biophys Res Commun. 2003; 305:278–286. [PubMed: 12745070]
37. Wang TS, Shu YF, Liu YC, Jan KY, Huang H. Glutathione peroxidase and catalase modulate the genotoxicity of arsenite. Toxicology. 1997; 121:229–237. [PubMed: 9231701]
38. Lu C, Qiu F, Zhou H, Peng Y, Hao W, Xu J, Yuan J, Wang S, Qiang B, Xu C, Peng X. Identification and characterization of selenoprotein K: an antioxidant in cardiomyocytes. FEBS Lett. 2006; 580:5189–5197. [PubMed: 16962588]
39. Panee J, Stoytcheva ZR, Liu W, Berry MJ. Selenoprotein H is redox-sensing high mobility group family DNA-binding protein that up-regulates genes involved in glutathione synthesis and phase II detoxification. J Biol Chem. 2007; 282:23759–23765. [PubMed: 17526492]
40. Gao Y, Hannan NRF, Wanyonyi S, Konstantopolous N, Pagnon J, Feng HC, Jowett JBM, Kim KH, Walder K, Collier GR. Activation of the selenoprotein SEPS 1 gene expression by pro-inflammatory cytokines in HepG2 cells. Cytokine+. 2006; 33:246–251. [PubMed: 16574427]
41. Ganyc D, Talbot S, Konate F, Jackson S, Schanen B, Cullen W, Self WT. Impact of trivalent arsenicals on selenoprotein synthesis. Environ Health Perspect. 2007; 115:346–353. [PubMed: 17431482]
42. Huang Z, Li J, Zhang S, Zhang X. Inorganic arsenic modulates the expression of selenoproteins in mouse embryonic stem cell. Toxicol Lett. 2009; 187:69–76. [PubMed: 19429247]
43. Margoshes M, Vallee BL. A Cadmium Protein from Equine Kidney Cortex. J Am Chem Soc. 1957; 79:4813–4814.
44. Albores A, Koropatnick J, Cherian MG, Zelazowski AJ. Arsenic induces and enhances rat hepatic metallothionein production in vivo. Chem-Biol Interact. 1992; 85:127–140. [PubMed: 1493605]
45. Freisinger E, Vasak M. Cadmium in metal-lothioneins. Met Ions Life Sci. 2013; 11:339–371. [PubMed: 23430778]
46. Ngu TT, Stillman MJ. Arsenic binding to human metallothionein. J Am Chem Soc. 2006; 128:12473–12483. [PubMed: 16984198]
47. Lipkowitz S, Weissman AM. RINGs of good and evil: RING finger ubiquitin ligases at the crossroads of tumour suppression and oncogenesis. Nat Rev Cancer. 2011; 11:629–643. [PubMed: 21863050]
48. Lipkowitz S, Weissman AM. RINGs of good and evil: RING finger ubiquitin ligases at the crossroads of tumour suppression and oncogenesis. Nat Rev Cancer. 2011; 11:629–643. [PubMed: 21863050]
49. Zhang XW, Yan XJ, Zhou ZR, Yang FF, Wu ZY, Sun HB, Liang WX, Song AX, Lallemand-Breitenbach V, Jeanne M, Zhang QY, Yang HY, Huang QH, Zhou GB, Tong JH, Zhang Y, Wu JH, Hu HY, de The H, Chen SJ, Chen Z. Arsenic trioxide controls the fate of the PML-RARa oncoprotein by directly binding PML. Science. 2010; 328:240–243. [PubMed: 20378816]

50. Ding W, Liu WL, Cooper KL, Qin XJ, Bergo PLD, Hudson LG, Liu KJ. Inhibition of poly(ADP-ribose) polymerase-1 by arsenite interferes with repair of oxidative DNA damage. J Biol Chem. 2009; 284:6809–6817. [PubMed: 19056730]
51. Zhou XX, Sun X, Cooper KL, Wang F, Liu KJ, Hudson LG. Arsenite interacts selectively with zinc finger proteins containing C3H1 or C4 motifs. J Biol Chem. 2011; 286:22855–22863. [PubMed: 21550982]
52. Bartel B, Wunning I, Varshavsky A. The recognition component of the N-end rule pathway. EMBO J. 1990; 9:3179–3189. [PubMed: 2209542]
53. Du FY, Navarro-Garcia F, Xia ZX, Tasaki T, Varshavsky A. Pairs of dipeptides synergistically activate the binding of substrate by ubiquitin ligase through dissociation of its autoinhibitory domain. Proc Natl Acad Sci U S A. 2002; 99:14110–14115. [PubMed: 12391316]
54. Rao H, Uhlmann F, Nasmyth K, Varshavsky A. Degradation of a cohesin subunit by the N-end rule pathway is essential for chromosome stability. Nature. 2001; 410:955–959. [PubMed: 11309624]
55. Ditzel M, Wilson R, Tenev T, Zachariou A, Paul A, Deas E, Meier P. Degradation of DIAP1 by the N-end rule pathway is essential for regulating apoptosis. Nat Cell Biol. 2003; 5:467–473. [PubMed: 12692559]
56. Kwon YT, Kashina AS, Davydov IV, Hu RG, An JY, Seo JW, Du F, Varshavsky A. An essential role of N-terminal arginylation in cardiovascular development. Science. 2002; 297:96–99. [PubMed: 12098698]
57. Tasaki T, Mulder LCF, Iwamatsu A, Lee MJ, Davydov IV, Varshavsky A, Muesing M, Kwon YT. A family of mammalian E3 ubiquitin ligases that contain the UBR box motif and recognize N-degrons. Mol Cell Biol. 2005; 25:7120–7136. [PubMed: 16055722]
58. Meisenberg C, Tait PS, Dianova II, Wright K, Edelmann MJ, Ternette N, Tasaki T, Kessler BM, Parsons JL, Kwon YT, Dianov GL. Ubiquitin ligase UBR3 regulates cellular levels of the essential DNA repair protein APE1 and is required for genome stability. Nucleic Acids Res. 2012; 40:701–711. [PubMed: 21933813]
59. Gozani O, Karuman P, Jones DR, Ivanov D, Cha J, Lugovskoy AA, Baird CL, Zhu H, Field SJ, Lessnick SL, Villasenor J, Mehrotra B, Chen J, Rao VR, Brugge JS, Ferguson CG, Payrastre B, Myszka DG, Cantley LC, Wagner G, Divecha N, Prestwich GD, Yuan JY. The PHD finger of the chromatin-associated protein ING2 functions as a nuclear phosphoinositide receptor. Cell. 2003; 114:99–111. [PubMed: 12859901]
60. Xiong L, Wang Y. Quantitative proteomic analysis reveals the perturbation of multiple cellular pathways in HL-60 cells induced by arsenite treatment. J Proteome Res. 2010; 9:1129–1137. [PubMed: 20050688]
61. Kobayashi A, Kang MI, Okawa H, Ohtsuji M, Zenke Y, Chiba T, Igarashi K, Yamamoto M. Oxidative stress sensor Keap1 functions as an adaptor for Cul3-based E3 ligase to regulate proteasomal degradation of Nrf2. Mol Cell Biol. 2004; 24:7130–7139. [PubMed: 15282312]
62. Kuhajda FP. Fatty acid synthase and cancer: new application of an old pathway. Cancer Res. 2006; 66:5977–5980. [PubMed: 16778164]
63. Vogel C, Marcotte EM. Insights into the regulation of protein abundance from proteomic and transcriptomic analyses. Nat Rev Genet. 2012; 13:227–232. [PubMed: 22411467]

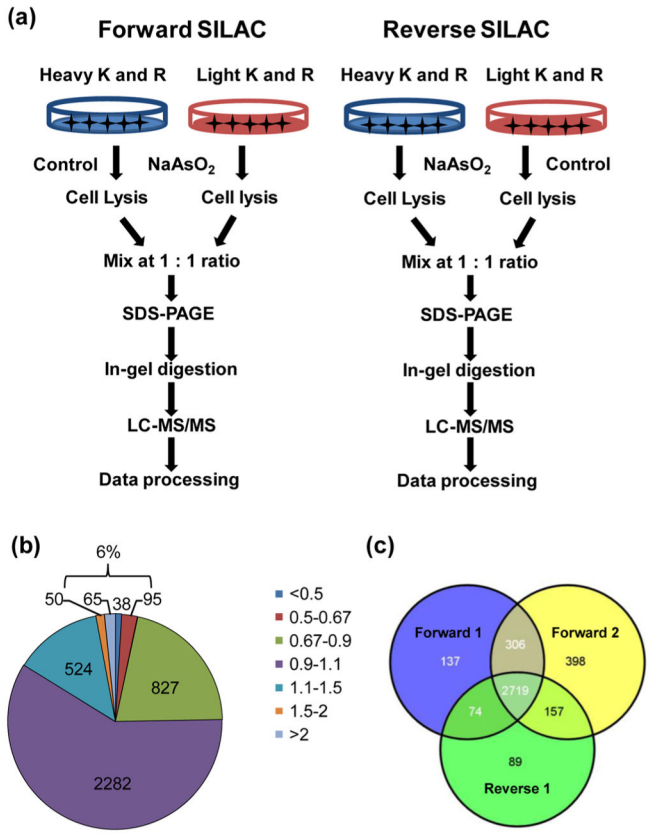


**Figure 1.**

Forward- and reverse-SILAC combined with LC/MS/MS for the comparative analysis of protein expression in GM00637 cells upon arsenite treatment (A). Pie chart displaying the distribution of expression ratios (treated/untreated) for the quantified proteins (B) and Venn diagram revealing the number of quantified proteins (C) from three independent experiments.

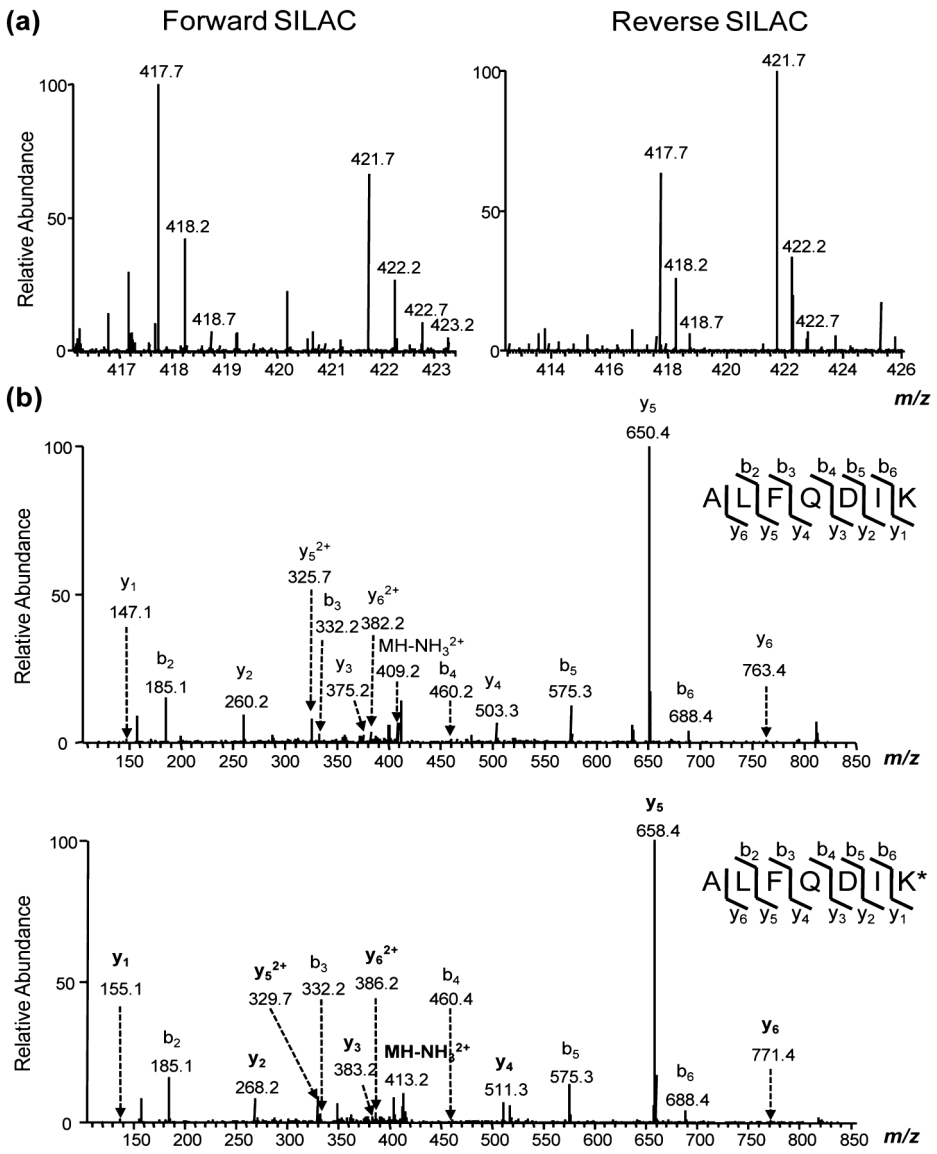


**Figure 2.**

Representative ESI-MS data revealing the arsenite-induced upregulation of ferritin. Shown are the MS for the $[M + 2H]^{2+}$ ions of ferritin peptide ALFQDIK (*m*/*z* 417.7) and ALFQDIK* (*m*/*z* 421.7)('K*' designates the heavy-labeled lysine) from the forward (left) and reverse (right) SILAC-labeling experiments (a) and MS/MS for the $[M + 2H]^{2+}$ ions of ALFQDIK and ALFQDIK* (b), where heavy-labeled lysine-containing y ions are labeled in bold.

## Table 1

A Select List of Significantly Changed Proteins Induced by Arsenite Treatment with the UniProt ID, Protein Names, and Expressions Ratios (Treated/Untreated, T/U)

| UniProt ID | protein name | ratio (T/U) (Mean ± S.D.) |
|---|---|---|
| | Nrf2-Related Proteins | |
| P09601 | Heme oxygenase 1 | 16.6 ± 2.6 |
| P02794 | Ferritin | 1.52 ± 0.02 |
| O75190-1 | DnaJ homologue subfamily B member 6 | 1.63 ± 0.59 |
| P50454 | 47 kDa heat shock protein | 1.52 ± 0.17 |
| P25685 | DnaJ homologue subfamily B member 1 | 1.53 ± 0.17 |
| Q9UDY4 | DnaJ homologue subfamily B member 4 | 1.46 ± 0.17 |
| O75190-1 | DnaJ homologue subfamily A member 1 | 1.39 ± 0.13 |
| P08107 | Heat shock 70 kDa protein 1/2 | 2.23 ± 0.47 |
| B3KTT5 | Highly similar to heat shock 70 kDa protein 1 | 2.30 ± 0.56 |
| P48507 | Glutamate–cysteine ligase modifier subunits | 2.18 ± 0.29 |
| P48506 | Glutamate–cysteine ligase catalytic subunits | 1.91 |
| P41743 | Atypical protein kinase C-lambda/iota | 2.4 ± 1.7 |
| P27986-4 | Phosphatidylinositol 3-kinase 85 kDa regulatory subunit alpha | 0.63 ± 0.34 |
| | Selenoproteins | |
| Q9Y6D0 | Selenoprotein K | 0.49 ± 0.08 |
| Q8WWX9 | Selenoprotein M | 0.33 ± 0.28 |
| Q8IZQ5 | Selenoprotein H | 0.64 ± 0.09 |
| Q9BQE4 | Selenoprotein S | 0.37 ± 0.08 |
| P36969-1 | Glutathione peroxidase 4 | 0.64 ± 0.06 |
| | Metallothioneins | |
| A8MWH4 | Metallothionein-1F | 2.43 ± 0.27 |
| P80294 | Metallothionein-1H | 2.97 ± 0.03 |
| P80297 | Metallothionein-1X | 6.57 |
| P02795 | Metallothionein-2 | 2.91 ± 0.15 |
| | Zinc-Finger Proteins | |
| Q99942 | E3 ubiquitin-protein ligase RNF5 | 0.66 |
| A8K901 | E3 ubiquitin-protein ligase UBR1 | 0.42 |
| Q6ZT12 | E3 ubiquitin-protein ligase UBR3 | 0.66 |
| Q8N806 | E3 ubiquitin-protein ligase UBR7 | 0.56 ± 0.06 |
| Q5BKZ1-1 | Zinc finger protein 326 | 2.2 ± 1.2 |
| O95159 | Zinc finger protein MCG4 | 1.64 ± 0.10 |
| | Cell Cycle Proteins | |
| Q13547 | Histone deacetylase 1 | 0.67 |
| Q96ST3 | Histone deacetylase complex subunit Sin3a | 0.48 ± 0.38 |
| O14519 | Cyclin-dependent kinase 2-associated protein 1 | 1.99 ± 0.39 |

## Table 2

Pathways Perturbed by Arsenite Treatment As Identified by IPA[a]

| Ingenuity canonical pathways | −log(p-value) | # of mol. | molecules |
|---|---|---|---|
| Pancreatic Adenocarcinoma Signaling | 3.38 | 7 | HMOX1 (16.54 ± 2.58), RAF1 (0.46), PLD3 (0.61 ± 0.16), PIK3R1 (0.63 ± 0.34), CDKN1A (0.43), ABL1 (5.57), SIN3A (0.48 ± 0.38) |
| NRF2-Mediated Oxidative Stress Response | 3.34 | 9 | HMOX1 (16.54 ± 2.58), PRKCI (2.44 ± 1.74), PIK3R1 (0.63 ± 0.34), DNAJB6 (1.63 ± 0.59), DNAJB1 (1.53 ± 0.17), GCLM (2.18 ± 0.29), FTH1 (1.52 ± 0.02), HSPA1 (2.23 ± 0.47), GCLC (1.91) |
| Chronic Myeloid Leukemia Signaling | 2.94 | 6 | RAF1 (0.46), PIK3R1 (0.63 ± 0.34), CDKN1A (0.43), HDAC1 (0.67), ABL1 (5.57), SIN3A (0.48 ± 0.38) |
| Fc$\gamma$ Receptor-Mediated Phagocytosis in Macrophages and Monocytes | 2.91 | 6 | HMOX1 (16.54 ± 2.58), ARF6 (0.61 ± 0.60), PLD3 (0.61 ± 0.16), PRKCI (2.44 ± 1.74), PIK3R1 (0.63 ± 0.34), RAB11A (2.91 ± 1.69) |
| Glioma Signaling | 2.89 | 6 | RAF1 (0.46), PRKCI (2.44 ± 1.74), PIK3R1 (0.63 ± 0.34), CDKN1A (0.43), ABL1 (5.57), SIN3A (0.48 ± 0.38) |
| G$\alpha$q Signaling | 2.58 | 7 | HMOX1 (16.54 ± 2.58), RAF1 (0.46), PLD3 (0.61 ± 0.16), PRKCI (2.44 ± 1.74), RND3 (1.60), PIK3R1 (0.63 ± 0.34), GNG5 (0.31 ± 0.04) |
| Cyclins and Cell Cycle Regulation | 2.52 | 5 | RAF1 (0.46), CDKN1A (0.43), HDAC1 (0.67), ABL1 (5.57), SIN3A (0.48 ± 0.38) |
| Aldosterone Signaling in Epithelial Cells | 2.49 | 6 | PLCD1 (0.63), RAF1 (0.46), PRKCI (2.44 ± 1.74), PIK3R1 (0.63 ± 0.34), DNAJB6 (1.63 ± 0.59), DNAJB1 (1.53 ± 0.17) |
| Prostate Cancer Signaling | 2.45 | 5 | RAF1 (0.46), PIK3R1 (0.63 ± 0.34), CDKN1A (0.43), ABL1 (5.57), SIN3A (0.48 ± 0.38) |
| PI3K Signaling in B Lymphocytes | 2.30 | 6 | ABL1 (5.57), MALT1 (3.43 ± 2.10), PIK3R1 (0.63 ± 0.34), PLCD1 (0.63), PRKCI (2.44 ± 1.74), RAF 1 (0.46) |
| Endothelin-1 Signaling | 2.25 | 7 | PLCD1 (0.63), HMOX1 (16.54 ± 2.58), RAF1 (0.46), PLD3 (0.61 ± 0.16), PRKCI (2.44 ± 1.74), PIK3R1 (0.63 ± 0.34), CASP14 (0.34) |
| ErbB4 Signaling | 2.19 | 4 | RAF1 (0.46), PRKCI (2.44 ± 1.74), YAP1 (0.64 ± 0.07), PIK3R1 (0.63 ± 0.34) |
| Cell Cycle: G1/S Checkpoint Regulation | 2.17 | 4 | CDKN1A (0.43), HDAC1 (0.67), ABL1 (5.57), SIN3A (0.48 ± 0.38) |
| Telomerase Signaling | 2.11 | 5 | RAF1 (0.46), PIK3R1 (0.63 ± 0.34), CDKN1A (0.43), HDAC1 (0.67), ABL1 (5.57) |
| Clathrin-mediated Endocytosis Signaling | 2.04 | 7 | LYZ (0.41), ARF6 (0.61 ± 0.60), APOB (0.58), PIK3R1 (0.63 ± 0.34), RAB11A (2.91 ± 1.69), S100A 8 (11.02), ARH (0.67) |
| IL-8 Signaling | 2.04 | 7 | HMOX1 (16.54 ± 2.58), RAF1 (0.46), PLD3 (0.61 ± 0.16), PRKCI (2.44 ± 1.74), RND3 (1.60), PIK3R1 (0.63 ± 0.34), GNG5 (0.31 ± 0.04) |

[a]The most statistically significant canonical pathways and molecules identified are listed according to their p-values. The threshold of the p-value is 0.05.